



Thermoluminescence study of the trapped charge at an alumina surface electrode in different dielectric barrier discharge regimes

P F Ambrico, M Ambrico, A Colaianni, L Schiavulli, G Dilecce, S de Benedictis

► To cite this version:

P F Ambrico, M Ambrico, A Colaianni, L Schiavulli, G Dilecce, et al.. Thermoluminescence study of the trapped charge at an alumina surface electrode in different dielectric barrier discharge regimes. Journal of Physics D: Applied Physics, 2010, 43 (32), pp.325201. 10.1088/0022-3727/43/32/325201 . hal-00569669

HAL Id: hal-00569669

<https://hal.science/hal-00569669>

Submitted on 25 Feb 2011

HAL is a multi-disciplinary open access archive for the deposit and dissemination of scientific research documents, whether they are published or not. The documents may come from teaching and research institutions in France or abroad, or from public or private research centers.

L'archive ouverte pluridisciplinaire **HAL**, est destinée au dépôt et à la diffusion de documents scientifiques de niveau recherche, publiés ou non, émanant des établissements d'enseignement et de recherche français ou étrangers, des laboratoires publics ou privés.

Thermoluminescence study of the trapped charge at alumina surface electrode in different dielectric barrier discharges regimes.

P F Ambrico¹, M Ambrico¹, A Colaianni^{2,4}, L Schiavulli^{3,4}, G Dilecce¹ and S De Benedictis¹.

¹ *Consiglio Nazionale delle Ricerche, Istituto di Metodologie Inorganiche e dei Plasmi UOS Bari - c/o Dipartimento di Chimica, via Orabona, 4, 70126 Bari, Italy*

² *Dipartimento di Geologia e Geofisica - via Orabona, 4, 70126 Bari, Italy*

³ *Dipartimento Interateneo di Fisica, - via Orabona, 4, 70126 Bari, Italy*

⁴ *INFN sezione di Bari, via Orabona, 4, 70126 Bari, Italy*

PACS 52.25.-b {Plasma properties}

PACS 52.25.Mq {Dielectric properties}

PACS 51.50.+v {Electrical properties}

PACS 78.60.Kn {Thermoluminescence}

PACS 72.20.Jv {Charge carriers: generation, recombination, lifetime, and trapping}

E-mail: paolofrancesco.ambrico@cnr.it

Abstract. In the present study charge trapping effect in alumina dielectric surfaces has been deeply investigated by means of a dedicated dielectric barrier discharge apparatus under different discharge regime and gas mixtures. These work further validates our previous findings in the case of air discharges under filamentary regime. The long lasting charge trapping has been evidenced by ex-situ thermoluminescence characterizations of alumina dielectric barrier plates exposed to plasma. The density of trapped surface charges was found to be higher in the glow discharge with respect to pseudoglow and filamentary regimes and for all regimes a minimum trap activation temperature was of 390 K and trap energy less than or around 1 eV. This implies that in the case of glow discharges a higher reservoir of electrons is present. Also, the effect was found to persist for several days after running the discharge.

1. Introduction

The surface charge trapping at dielectric surface due to exposure to atmospheric pressure dielectric barrier discharge (DBD) plasma can influence the discharge regime [1]; in fact surface charges act as a reservoir that can contribute to stabilize a glow discharge regime for instance in air discharges [2]. Golubovskii et al. suggested that many seed electrons necessary for a uniform/homogeneous discharge could be produced by electrons trapped on the dielectric surface [3]. Recently, long lifetime of charge trapping on alumina used as dielectric in DBD plasma has been evidenced by Thermally stimulated current [1] and Thermoluminescence technique [4]. We found that the adsorbed electrons in the case of alumina were trapped in shallow traps during plasma running and have mainly an energy of about 1eV [4], i.e. at a much lower energy than the intrinsic alumina electrons and much easier to be removed from the dielectric. These trapped electron could

also explain the fact that irradiating the dielectric surface with low fluence laser beam could result in the triggering of a discharge for a voltage lower than the breakdown value [5].

From what stated above, it follows that different discharge regimes are expected to act differently on the surface charge trapping since the plasma electron energy distribution and current can be different. It is also furthermore known that DBD can run under filamentary or diffuse mode depending on discharge geometry and gas mixture. For instance, the nitrogen discharge can be run in different regime depending on the geometry and other discharge parameters[6,7]. Moreover, the addition of small quantities of oxygen to a nitrogen discharge transform the regime from glow to filamentary [8]. Conversely, running an helium discharge this will lead to a quite distinct glow regime [9].

The aim of this work is to study the surface charge trapping effect under different discharge regime and gas mixture at atmospheric pressure running in a dedicated experimental set up. The effect of surface charge trapping on the dielectric barrier plates after plasma exposure will be evidenced by ex-situ Thermo Luminescence glow curve (TL GC) measurements as already preliminarily described in ref.4. The correlation between the discharge regimes and the observed glow curves parameters will be discussed.

2. Experimental

A DBD discharge apparatus has been build up in order to easily control the surface area exposed to the plasma; respect to previous experimental configuration [4], each single specimen of alumina (mean diameter 0.5 mm), constitute one of two dielectric barrier plates, covering the metallic electrodes, exposed to plasma. A drawing of the discharge apparatus is shown in figure 1.

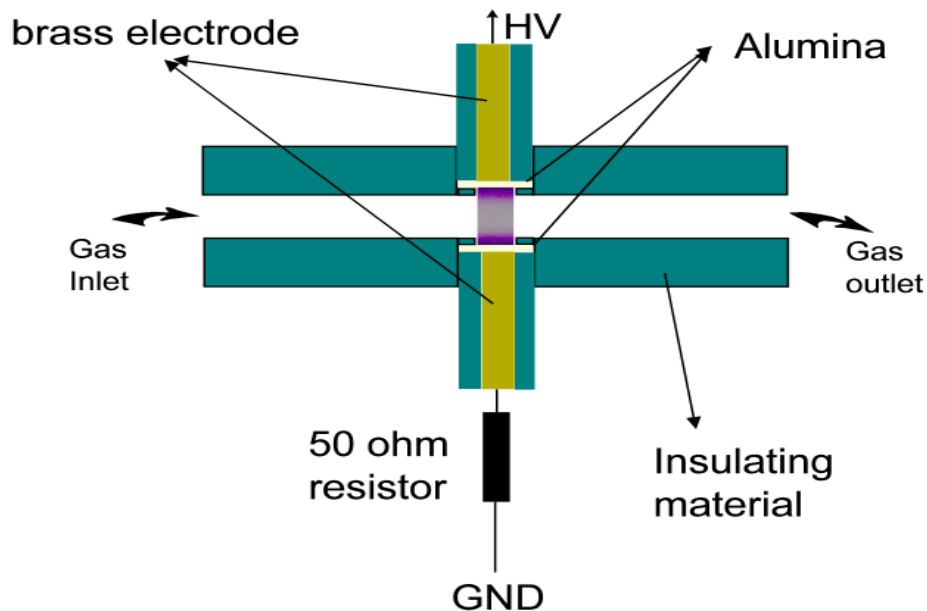
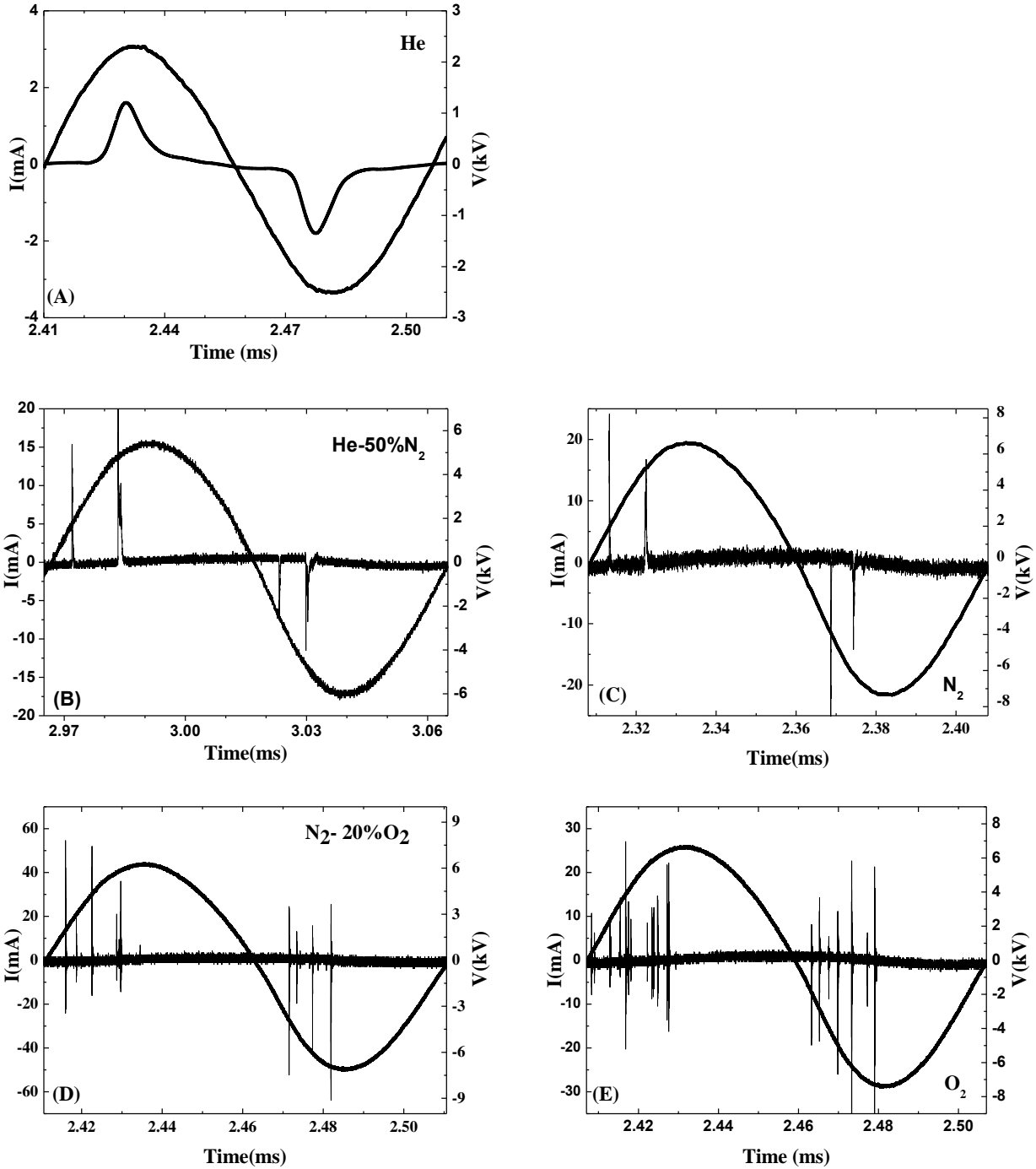


Figure 1. Schematic of the experimental apparatus (colour online).

The parallel plates discharge is composed of two brass electrode 3 mm in diameter, two 0.7 mm thick alumina plates (Coorstek fine grain, 96% purity) that completely cover the electrodes and two spacers designed to vary the discharge gap from a minimum of 2 mm (for N₂ main gas mixtures) and 5 mm for He

main gas mixtures. The minimum distance between electrodes is limited by the geometry of the electrode support. The electrodes are completely isolated by highly insulating plastics except the surface in contact with the aluminum dielectrics. The discharge vessel is made of a stainless steel and PVC flanges for the high voltage (HV) connections and is equipped with vacuum fittings.

Figure 2. Typical voltage and current waveforms for: (A) He, (B) He-50%N₂, (C) N₂, (D) N₂-20%O₂, (E) O₂ plasmas.



Before operation the discharge volume is evacuated to few tens of mTorr by a 30 m³/h rotary pump. The gas flow is operated by MKS flow meters/controllers, and pumping through an adjustable needle valve is used to maintaining the 760 Torr pressure under a total gas flow of 1000 sccm. Pure N₂, O₂ and He (impurities less than 6 ppm) are used as gases supply. The HV supply is composed of a low voltage sinusoidal generator

(Wavetek mod. 164), a power amplifier (Industrial Test Equipment Powerton 1000A), and a high voltage transformer. The applied voltage is pulse modulated with duty cycle $T_{on}=T_{off}=5\text{ms}$. Different discharge regimes have been produced under different plasma mixture. Specifically, a filamentary regime will be typical of N_2 - 20% O_2 (air like mixture) and O_2 discharge, a diffuse range will characterize that of He while an intermediate regime will be that of N_2 and He- 50% N_2 discharges. The discharge parameter, current and voltage, have been continuously monitored and registered during each run. Typical oscillograms of the applied voltage and discharge current for DBD for a total pressure of 760 torr, flow rate of 1 liter/minute and different gas mixture area reported in figure 2.

The discharge regimes characterizing the working conditions of DBDs in the present study are shown in figure 2. In the case of Helium discharges, the DBD is homogeneous/diffuse along the plane of the electrode and in the discharge gap. The glow character is associated to one major current peak for half cycle. The discharge in nitrogen and nitrogen helium is homogeneous and assume the pseudoglow [10] discharge aspect, with usually a first current pulse which has a faster rise time and shorter duration, and a second pulse in both polarities which has not only an appreciably longer rise time but also a rather long decay time constant. Both current peak have a pulse duration of few microseconds. In the case of air and oxygen the discharge is in a filamentary state that is consisting of a large number of narrow filaments stochastically distributed over the electrode area. The discharge current has the form of multiple peaks (micro-discharges) of some tens of nanosecond duration.

From the current measurements the electron current transferred charge can be estimated by the integration of the current peak, using $Q=\int i(t)dt$ for a current peak recorded in single-shot after subtraction of the displacement current. Of course the charge measured using this method is generally slightly underestimated [11] in the case of filamentary regime, in which faster signal are involved and the oscilloscope sampling can be affected by higher error. Since the current for one cycle is monitored continuously an average transferred charge per cycle can be easily estimated, and the total current transferred charge can be estimated by multiplying it for the total number of cycles during the measurements period.

During all the experiments several alumina disk plates ($\varnothing = 6 \text{ mm}$ and 0.7 mm thick) taken from the same $7 \times 7 \text{ cm}^2$ slabs were used as dielectric barrier of ground electrode so to be easily removed after discharge run and analysed ex-situ by TL apparatus.

The thermoluminescence glow curves were collected on alumina samples gas plasma by using an automated RISØ TL/OSL-DA-15 [12] reader equipped with $^{90}\text{Sr}/^{90}\text{Y}$ beta (β) source radiation (0.565 MeV mean β energy, dose rate 0.119 Gy/s). The system is equipped with a photomultiplier tube (bi-alkali EMI 9235QA), which has a maximum detection efficiency at approximately 400 nm, at a distance of 55 mm from the sample. The spectral selection was accomplished by means of a 7.5 mm Hoya U-340 detection filter ($\lambda_{\text{peak}} = 340 \text{ nm}$, FWHM = 80 nm).

The thermoluminescence glow curves have been acquired by heating the sample in an inert nitrogen atmosphere (2 liter/minutes flow) at a heating rate of 5K/s in the temperature range 323K – 673K . The measurement is accomplished in 90 seconds.

119 All the alumina samples were preliminarily classified (after thermal annealing at 800°C for two hours) by
 120 means of Thermoluminescence measurements, that was used as reference for the sample, following a typical
 121 radiation dosimetry protocol:

- 122 a) thermoluminescence background;
- 123 b) 90 s beta irradiation;
- 124 c) thermoluminescence glow curve;

125 Before each plasma exposure the alumina disks were thermally cleaned at 800°C for two hours, in order to
 126 deplete spurious trapped charges due to exposure to environmental radiation.

127 After plasma exposure the alumina disks have been promptly dismantled in dark conditions stored in a black
 128 box, to avoid or reduce any possible thermo luminescence glow curve intensity reduction due to bleaching
 129 effect, in dry air and mounted in the TL apparatus. The overall time from the switch off of the plasma to the
 130 start of the Thermoluminescence measurements was about 20 minutes. The Plasma induced luminescence
 131 [13] counts at the beginning of the measurements in the UV region covered by the TL filters were negligible.
 132 The Thermoluminescence protocol after plasma exposure was the following:

- 133 a) Thermoluminescence readout (that takes about 90 seconds);
- 134 b) Thermoluminescence background. In all the sample after different plasma exposure the collected
 135 background was comparable to the reference indicating that no luminescence was coming from the sample
 136 after the thermoluminescence signal readout. We can exclude thermally activated reaction from the surface
 137 as reported in [13] .
- 138 c) Control Thermoluminescence readout following the beta radiation exposure protocol. For all the samples
 139 the beta irradiated thermoluminescence were always very close to the control one collected at the beginning.
 140 This is an indication that the surface was not modified by the plasma or for beta radiation damage or
 141 sensitization.

142 Plasma exposure times have been varied ranging from 5 to 90 minutes in the case of air discharge and from 5
 143 to 30 minutes in the case of He and He N₂ discharges. In the case of He two different high voltage values (3
 144 kV_{pp} and 5 kV_{pp}) were used that is leading to different discharge current. As a matter of comparison,
 145 thermoluminescence glow curves were also collected on a set of alumina samples after β exposure and
 146 varying the irradiation time from 60s to 2100s i.e. for a total dose ranging from 7 Gy to 250 Gy.

147 The thermoluminescence glow curves have been analyzed by using the free downloadable GLOW FIT
 148 program [14] capable of simultaneously processing up to ten TL glow peaks following the first order kinetics
 149 model [15].

150

151 **3. Results and discussion**

152 *3.1 The thermoluminescence technique*

153 The charge trapping effect due to plasma exposure was approached by using the thermoluminescence
 154 properties of the dielectric plates used as barrier in DBD discharge. It could be useful to remind that in a pure
 155 insulator (but this hold also for semiconductors) there are two relevant energy bands: (i) an almost

completely filled valence band and (ii) an almost empty conduction band separated by a forbidden gap (called band-gap energy E_g). Transitions of electrons between the valence band and the conduction band can occur if the valence band electron acquires an energy $\geq E_g$.

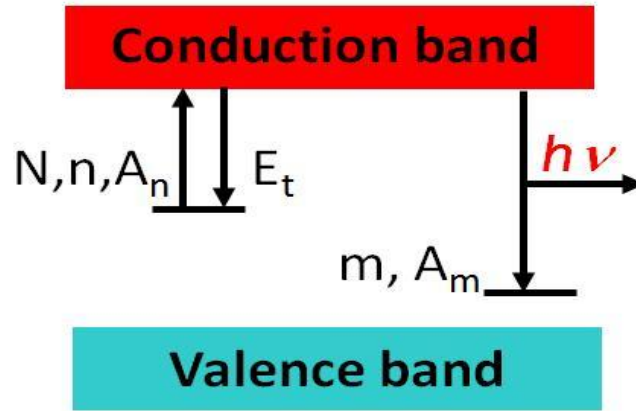


Figure 3. Scheme of principle of charge trapping/detrapping and recombination mechanisms in an insulating material leading to a luminescence (or thermoluminescence) effect. Here the simplest case on one trap and one recombination center energy distribution are displayed. N is total trap state concentration, n the concentration of trapped electrons; m is concentration of available hole states (for recombination); E_t is the trap energy; A_n is the retrapping probability and A_m is the recombination probability (colour online).

Imperfections in the crystal, associated with impurities and/or lattice defects may create new localized energy levels in the forbidden band gap. Under certain conditions, some of these defects are capable to trap an electron. One of this conditions is ionizing radiation exposure producing free electrons that can be trapped on one of more than of these sites. Some of these traps can be thermally depleted and recombine on recombination centers emitting a photon. This is the basic phenomenon on which the thermoluminescence technique works. The trap determined after a TL measurements is characterized by the energy E_t (which is referred to as the trap depth) that an electron must acquire from lattice vibrations to escape to the conduction band where it can move freely in the crystal and by the characteristic temperature T_m at which the thermal vibrations of the crystal lattice are sufficient to cause the release of trapped electrons. The rate at which the electrons, or holes, escape from the traps is roughly governed by the vibrational frequency (or attempt-to-escape factor or frequency) s of the charge within the trap and the trap depth E . The overall escape rate is proportional to $S \cdot \exp(-E_t/kT)$.

The thermally stimulated light emission from an insulator or a semiconductor following the previous absorption of energy from ionizing radiation results in the typical Thermoluminescence glow curve from which the information on the electron traps present in the band gap can be extracted. By looking at Figure 3, under the hypothesis that the total electron retrapping probability $(N-n)A_n$ is much lower than the recombination probability mA_m (i.e. slow retrapping condition), the thermoluminescence intensity for single peak is given by the well known first order kinetic equation [16] in the case of a linear temperature gradient:

$$I(T) = n_0 S \exp\left(-\frac{E_t}{kT}\right) \exp\left(-\frac{S}{\delta} \int_{T_0}^T \exp\left(-\frac{E_t}{kT'}\right) dT'\right) \quad (1)$$

Where δ is the heating rate, T_0 is the initial temperature, n_0 the initial number of filled traps, E_t is the trap energy, S is the above expressed frequency factor (s^{-1}) indicating also the number per second an electron interacts with the lattice. The exponential integral in equation (1) could be only analytically solved [17] and gives a representation of the single peak glow curve as a non linear function of trap energy E_t , peak temperature at maximum T_M and peak maximum intensity I_M . The integral in (1) is then the representation of a glow peak with a maximum intensity I_M at a characteristic temperature T_M following the equation:

$$\frac{\delta E_t}{kT_M^2} = S \exp\left(-\frac{E_t}{kT_M}\right) \quad (2)$$

It then follows that the integral light intensity depends on the number of trapped charges that are in turn depending on the irradiation dose and independent on the heating cycle. The characteristic temperature T_M does not depend on the number of trapped charges and relates with the trap energy E_t .

Moreover, the trap energy depth E_t , the peak maximum temperature T_M and the width of the peak ω (defined as the ratio A/I_M i.e. between the glow peak area and the peak intensity at its maximum), are related among them by the following relation [18]:

$$E_t \cong \frac{kT_M^2}{\omega} \quad (3)$$

From eq.(3) it should be expected that glow peak at higher temperature correspond to deeper traps. However, when complex glow curve resulting from peak overlapping are analyzed this is not a followed rule since also the width of glow peak contributes in defining the correspondence between the energy and glow peak maximum temperature[18]

The analysis of such complex curves can be nowadays afforded by a friendly free downloadable software namely GlowFit program [14] specially designed to simulate thermoluminescence glow curve resulting from up ten single or superimposed glow peaks following the first order kinetics. The GlowFit software allows to determine the trap energy depth E_t , the peak maximum temperature T_M , the peak maximum intensity I_M and the frequency factor S as *output* best fit parameters and calculates the peak area A . Moreover, the goodness of the fit is expressed through the figure of merit (FOM) value that is a further program output and is defined as :

$$FOM(\%) = \sum_{i=1}^n 100 \cdot \frac{|\Delta y_i|}{A_T} \quad (4)$$

where n is the number of data points, Δy_i is the difference between the experimental and fitted points and A_T is the integral of the fitted glow curve in the region of interest [19].

3.2 Effect of different discharge regimes

In figure 3 the collected thermoluminescence glow curves (TL GCs) for a 30 minutes plasma exposure time and different gas mixture discharges and GC referred to 90 seconds β exposure are reported. In analogy to

the terminology used for the β radiation, we will refer to “plasma radiation” as the sum of all agents (electrons, photons, ions) that, impinging on the dielectric, are capable to excite an electron into a surface trap level and term “plasma radiation dose” the corresponding estimated dose.

The TL GC intensity of the different observed spectra shown in figure 4 relates well with the measured current in the different plasma regime conditions. In fact the higher electron current transferred charge is obtained in the helium plasma glow regime, then the pseudo-glow regime of helium-nitrogen and nitrogen plasma and last the filamentary regime of air and oxygen plasma (see table 1).

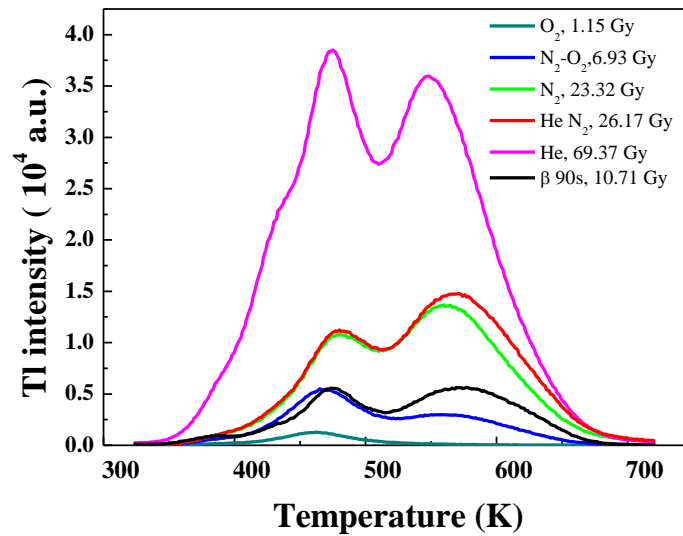


Figure 4. Thermoluminescence glow curves after alumina exposed to different gas mixture discharge plasma. The GC data refers to 30 minutes plasma exposure. Glow curve after 90 s of β exposure is also shown for comparison. (colour online)

It is evident that exposing the alumina samples for the same time to different plasma produces thermoluminescence glow curves with different intensities. Furthermore, the plasma induced thermoluminescence glow curves display features similar to those observed after β irradiation which is constituted of high energetic electron current. Possible effects of the alumina exposure to UV radiation although present in the plasma as irradiation source have been excluded since, as previously observed, glow curve observed after UV (mercury lamp) exposure display a different shape due to the UV light induce bleaching effect [4]. Respect to previously published results for the case of synthetic air [4], referring to glow curve collected after some days from plasma exposure, the short delay between the N_2 - O_2 plasma exposure and thermoluminescence measurements results in a much more intense glow curve.

The radiation dose after plasma exposure was estimated by using the known β radiation source dose rate as a reference. First of all the linear dependence of the thermoluminescence glow curve area on the total β radiation dose has been verified (see figure 5)

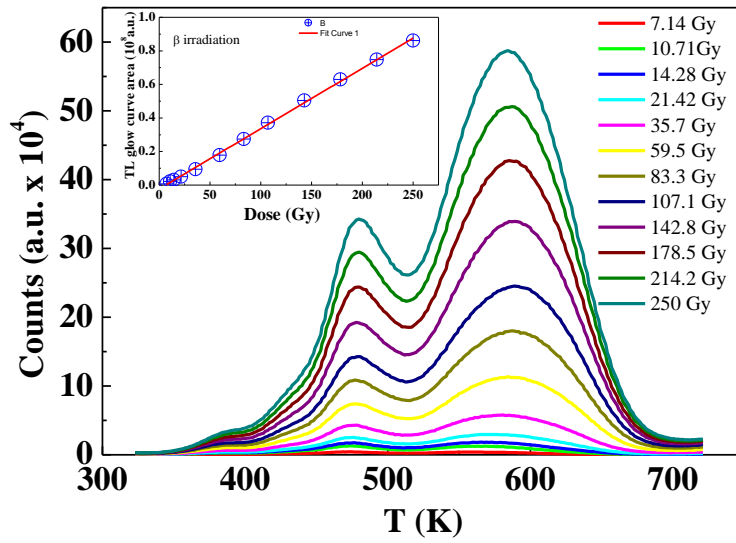


Figure 5. Thermoluminescence glow curves for different β radiation exposure time (i.e. total dose). The alumina sample response is linear with the dose. (colour online)

Therefore, it has been possible to estimate the total plasma exposure dose from the ratio of the plasma thermoluminescence glow curve area and the β thermoluminescence glow curve area for a given radiation dose (i.e. 10.7 Gy). To minimize the experimental error on the plasma radiation dose estimate the reference signal obtained after exposure to the β radiation source were collected on each sample after collecting the plasma thermoluminescence glow curve. The experimental error can be due to small differences on the geometrical area of the alumina slabs or to different GC intensities produced by β irradiation due to sensitization effects. The reference signal enable us also to verify that no radiation damage or sensitization effect was produced on the dielectric surface.

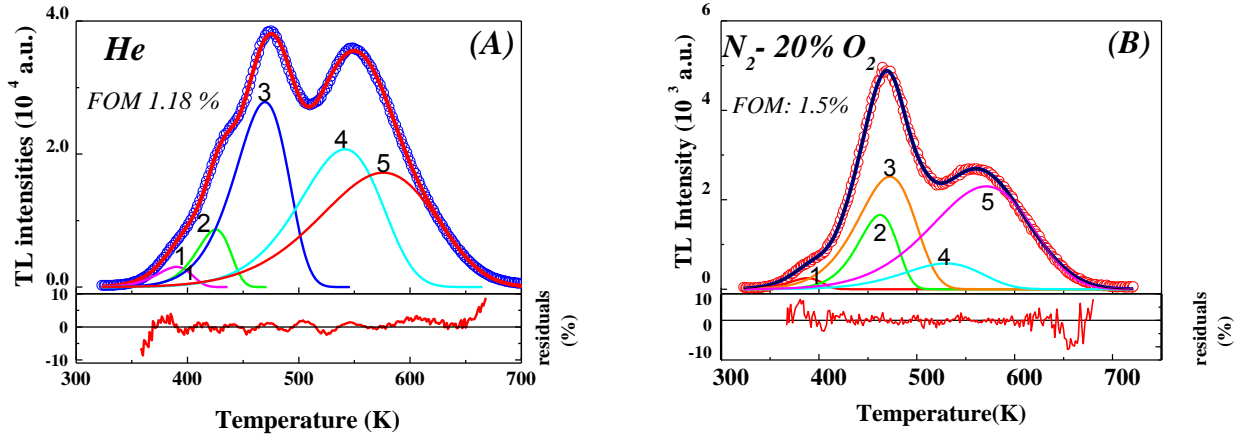
The total plasma radiation dose for the different discharges are reported in Table 1. As can be observed, He plasma is highly effective in filling several traps in the overall thermoluminescence temperature range while the O_2 plasma is the least effective one. It must be however pointed out that despite the not so much different current from the case of N_2 - O_2 discharge the number of counts observed in O_2 plasma produced glow curve is smaller. The counts reduction observed in O_2 discharge can be ascribed to the presence of an higher level of ozone producing de-trapping effect associated to the ozone-surface interaction. It has been in fact demonstrated that ozone annealing efficiently eliminates the charge trapped in the dielectric used as capacitor material [20].

<i>PLASMA</i>	<i>PeakN[°].</i>	<i>T_m</i> (K)	<i>E_t</i> (eV)	<i>Peak Area</i> (a.u.)	<i>S</i> (s ⁻¹)	<i>ω</i>	<i>Dose</i> (Gy)	<i>E_{Ton}</i> (mJ)	<i>Q_{cycle}</i> (C)
<i>O₂</i> <i>FOM</i> <i>2.37%</i>	<i>1</i>	390	0.755	2310	1.60 10 ⁹	27	1.15	8.9	1.4 10⁻⁹
	<i>2</i>	458	0.888	20803	1.46 10 ⁹	32			
	<i>3</i>	474	0.608	27687	4.61 10 ⁵	48			
	<i>4</i>	520	0.562	9353	3.71 10 ⁴	61			
	<i>5</i>	575	0.500	4064	2.12 10 ³	83			
<i>N₂-O₂</i> <i>FOM</i> <i>1.5%</i>	<i>1</i>	388	0.756	6550	3.79 10 ⁹	27	6.93	6	2 10⁻⁹
	<i>2</i>	462	0.890	53984	2.42 10 ⁹	32			
	<i>3</i>	473	0.620	118712	1.32 10 ⁶	47			
	<i>4</i>	530	0.562	36862	5.12 10 ⁴	64			
	<i>5</i>	571	0.500	188080	4.62 10 ³	82			
<i>N₂</i> <i>FOM</i> <i>1.76%</i>	<i>1</i>	388	0.852	11418	7.84 10 ¹⁰	38	23.32	12	9 10⁻⁹
	<i>2</i>	418	0.99	12574	5.72 10 ¹¹	24			
	<i>3</i>	475	0.759	290354	4.36 10 ⁷	40			
	<i>4</i>	552	0.703	344381	6.78 10 ⁵	57			
	<i>5</i>	580	0.500	701399	3.79 10 ³	84			
<i>He-N₂</i> <i>FOM</i> <i>1.68%</i>	<i>1</i>	390	0.868	12425	5.40 10 ¹⁰	23	26.17	5.9	1.1 10⁻⁸
	<i>2</i>	422	1.090	15618	3.63 10 ¹²	22			
	<i>3</i>	475	0.770	296911	2.87 10 ⁷	39			
	<i>4</i>	559	0.622	432134	4.71 10 ⁴	64			
	<i>5</i>	587	0.500	769263	1.66 10 ³	86			
<i>He</i> <i>FOM</i> <i>1.18%</i>	<i>1</i>	390	0.810	77232	1.77 10 ¹⁰	25	69.37	7.55	2.8 10⁻⁸
	<i>2</i>	425	0.991	216310	3.50 10 ¹¹	25			
	<i>3</i>	470	0.758	1080551	5.47 10 ⁷	38			
	<i>4</i>	542	0.638	1235783	2.20 10 ⁵	59			
	<i>5</i>	576	0.500	1430699	4.15 10 ³	83			

Table 1. Best fit parameters extracted using the GlowFit program, i.e. Peak Temperature T_m (K); Trap Energy E_t (eV); Peak Area, A (a.u.); Frequency factor, s (s⁻¹); Figure of Merit (FOM). The peak width ω and Dose (Gy) are calculated as described in the text. The fitted glow curves refers to 30 minutes plasma exposure for gas mixture plasmas leading to different discharge regime. In the table are reported the corresponding plasma macroscopic parameters i.e.: Energy T_{on} (mJ); plasma current charge per cycle Q_{cycle} (C).

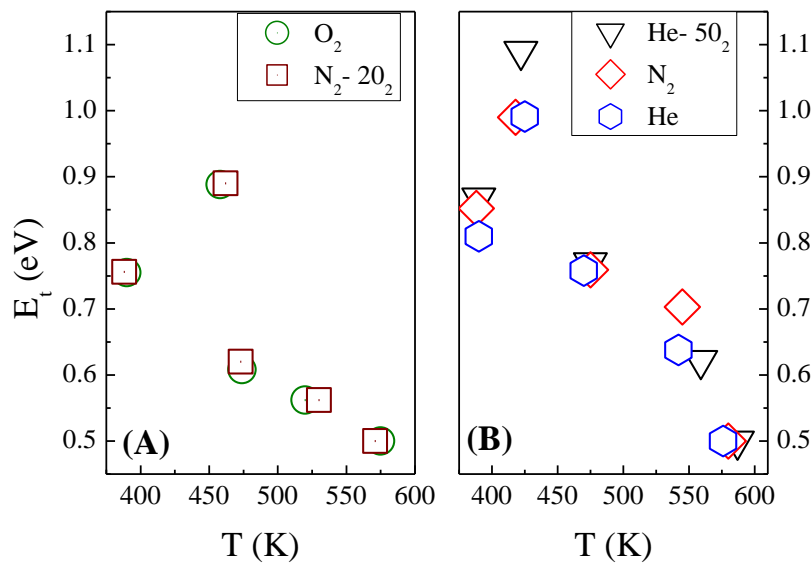
The peak deconvolution procedure [14] helps to better elucidate on the plasma radiation thermoluminescence glow curve features and involved trap energies. In figure 6 the deconvolution for the thermoluminescence

273 glow curve obtained after He and air discharge are reported as examples together with the residual and the
 274 figure of merit (FOM) for each fit.



275
 276 **Figure 6.** Glow curve fitting curve (red straight line) and deconvoluted peaks resulting as the output of the application
 277 of the GlowFit software on the experimental thermoluminescence curve (circles) for He (a) and N₂ O₂ (synthetic air,
 278 (b)). The TL GC refers to 30 minutes plasma exposure. In the bottom part the residual values in the examined
 279 temperature range have been represented. The residual represents the difference at each temperature between the
 280 experimental and fitted points in the GC. The FOM values have been also reported. (colour online)

281
 282 The best fit parameters obtained after peak deconvolution, referring to each peak, have been listed in Table 1
 283 and represents the thermoluminescence glow peak maximum temperature (T_m), trap activation energies (E_t),
 284 frequency factor S , glow peak area (A) and figure of merit values (FOM)[21]. The frequency factor s and has
 285 been found higher for the lowest temperature peaks. The FOM accounts for the goodness of
 286 thermoluminescence glow curve modeling and respect to previously published results [4], the fitting
 287 procedure has been improved by reducing the figure of merit (FOM) values less than 2% (see Table 1).



288
 289 **Figure 7.** Correlation between the discharge regimes and the deconvoluted peak parameters (T_M and E_t) of Table 1:
 290 filamentary regimes (A) and glow and pseudo glow regimes (B). (colour online)

291

292 The deconvolution of glow curve produced after plasma exposures evidence five contributing peaks. The
 293 results reported in Table 1 can be more easily understood if we consider figure 7.

294 It can be observed that traps filled by the plasma are similar in the case of air and oxygen discharge, but with
 295 a trapping efficiency higher for the air like plasma (see Table 1). We speculate that in N₂-O₂ plasma the
 296 lower ozone production leads to a lower ozone-mediated detrapping effect.

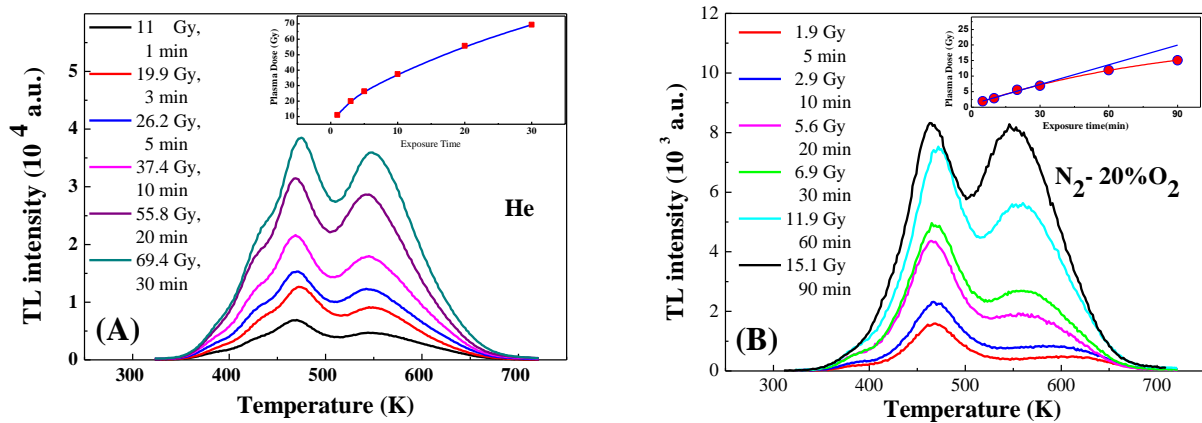
297 The glow curve intensities produced in the case of glow (He) and pseudo glow (N₂, He-N₂) regime show
 298 very strong similarities. In particular the higher temperature peaks are the same with slight differences in the
 299 peak temperatures (< 15K) and energies (< 10 meV). These attributions are furthermore justified when
 300 considering the similar order of magnitude of the frequency factor *S* values.

301 We can conclude that the different discharges characterized by different regimes (i.e. different plasma
 302 current and electron energy) are more or less effective in filling the electron traps in the dielectric materials.
 303 We can also speculate that the trap filled by different plasmas are keeping memory of the active species
 304 (metastable, or electronegative gases, etc.): in fact different trap at dielectric surface are filled giving a
 305 different signature on the thermoluminescence glow curve.

306

307 3.3 Effect of the exposure time

308 The thermoluminescence glow curves were collected for different total exposure time of the alumina samples
 309 to He and N₂-O₂ plasmas, in order to observe the effect of two extreme plasma regimes (glow and
 310 filamentary respectively) on charge trapping. In figure 8 the obtained glow curves are reported together with
 311 the estimated dose for the different exposure time.



312

313 **Figure 8.** Thermoluminescence glow curves for different time exposure in the case of (a) Helium and air (b) discharge.
 314 In the legend the estimated total dose are reported together with the total exposure time. (colour online)

315

316 At the lowest doses, the thermoluminescence glow curve intensity is higher in the lower temperature region
 317 than in the high temperature region. Increasing the exposure time the thermoluminescence glow curve
 318 intensities for the two temperature region seem to converge to an almost common value. This effect is due to
 319 the presence of several trapping states that can act one as active and other as competitor traps. Generally, the

trapping probability of the competitor trap is higher than that of the active one so that the glow peak area tends to saturate due to the fast filling of competitor trap levels; after competitor level saturation more electrons are trapped to the active states that shows a fast linear trap filling [15]. These effects may account for the behavior observed at the lowest doses in He and air discharge.

In the inset of figure 8 are represented the total thermoluminescence glow curve area values as a function of irradiation time, that in the case of beta irradiation can be easily converted in the total radiation dose. A saturation effect is clearly observed in He while in N₂-O₂ it is less marked. It has to be stressed that saturation effect has not been observed after β irradiation both for doses similar or much higher than plasma ones.

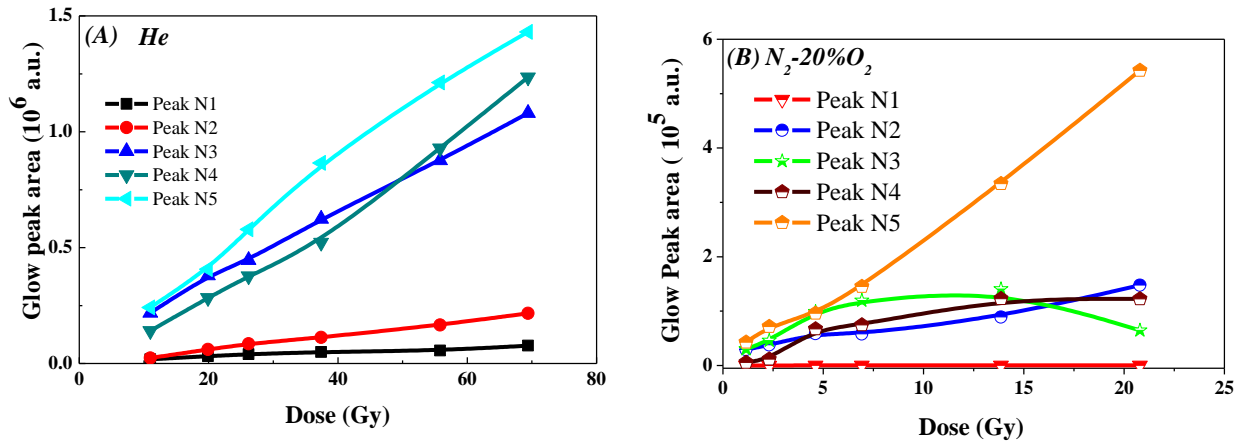
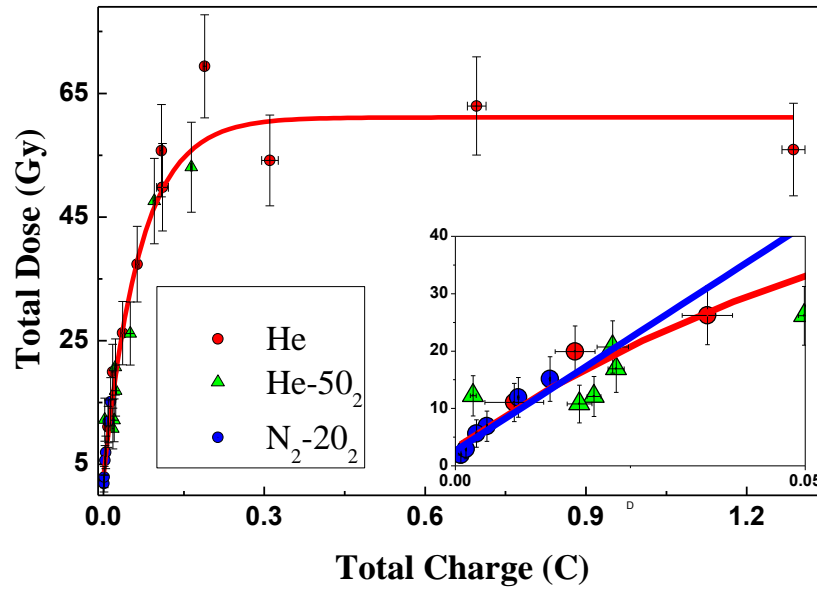


Figure 9. Thermo luminescence deconvoluted glow curve peak areas versus plasma dose for the case of He (a) and Air like plasma (b) discharge. N.i. represent the peak number as reported in Table 1. (colour online)

The dynamic behavior of thermoluminescence glow curve has been exploited by examining the evolution of each glow peak when changing the plasma doses. It has to be underlined that since plasma dose depends on the discharge regime, the examined dose range is different although exposure time is the same. Figure 9 shows the glow peak areas as a function of the corresponding irradiation dose under glow (He figure 9(a)) and filamentary (N₂-O₂ (figure 9(b)) discharge regime. In the glow regime, the lower temperature and the highest temperature peak areas saturates(competitor traps), while intermediate temperature peak display a general linear behavior (active trap). In the filamentary regime, the highest temperature peak display an almost linear behavior (active trap) while the remaining peaks saturate with the dose (competitor trap).

The overall saturation effect observed in the case of plasma induced charge trapping can be explained if we consider that the plasma electron energy is typically of the order of a few eV, i.e., five orders of magnitude lower than the beta source, leading to an electron penetration depth of around tens of nanometer [22]. Therefore the plasma electrons are effective mostly on the first monolayers of alumina surface where they are readily stopped rather than on the overall bulk, which is instead fully crossed by beta radiation. This means that the real volume of the sample that is irradiate by plasma is smaller. If we assume that the traps are randomly distributed in the sample this means that the number of traps that can be filled by the plasma radiation is considerably lower, and as a consequence the saturation dose is also lower [23]. This is

349 furthermore confirmed by comparing the glow curve area vs dose collected after β and plasma irradiation in
 350 the same dose range (up to 50 Gy) that was found linear for the former while saturates for the latter.
 351 The strong correlation between the estimated plasma radiation dose and the plasma current is evidenced in
 352 figure 10. Several experiment were run for different gas mixtures and regime in He, He/N₂, N₂, N₂/O₂, the
 353 current was constantly monitored and the thermoluminescence measurements performed soon after each run,
 354 together with the corresponding calibration measurements by irradiation with β radiation.

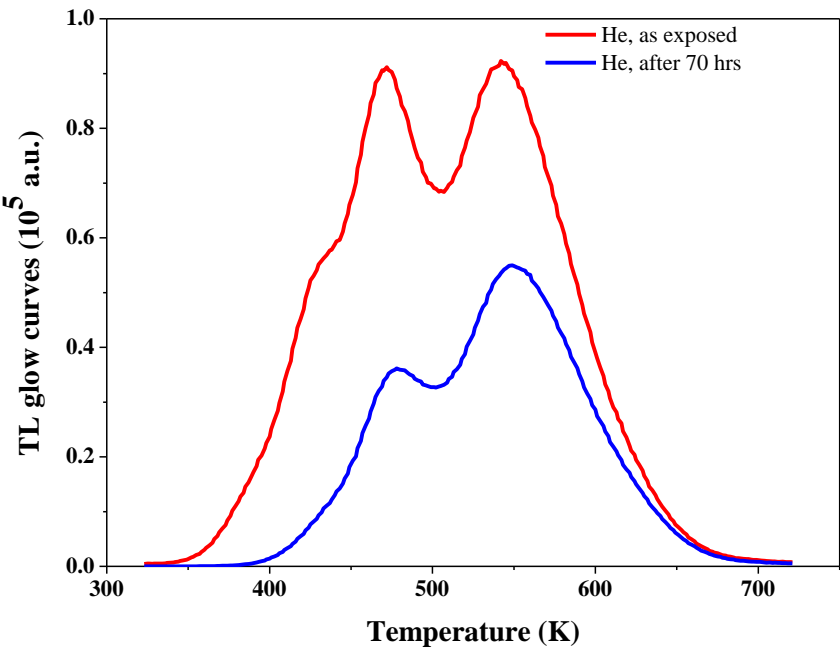


355
 356 **Figure 10.** Estimated total doses for different plasmas as a function of the total discharge current estimated charge. The
 357 dose is linearly proportional to the charge up to dose of 15 Gy and deviates from linearity for higher doses, as observed
 358 when plotting the dose as a function of time exposure. (colour online)
 359

360 For values of the total dose less or equal to 11 Gy the plasma radiation dose is linearly correlated to the total
 361 current transferred charge estimated by the integration of the current peak, while start to show a saturation
 362 effect for higher dose rate. In particular saturation is easily reached in the case of Helium, and He N₂ gas
 363 mixture. If we look carefully at figure 10 we can observe that if the estimated total plasma current transferred
 364 charge is the same, then estimated plasma radiation dose is also the same. This can be a further indication
 365 that the electrons hitting the surface are the main responsible for the charge trapping. Moreover the observed
 366 charge trapping generated by plasma exposure is a long lasting effect. A set of dedicated experiment was run
 367 in the case of He discharges in order to clearly show this effect.

368 Figure 11 is an example of the time evolution of the thermoluminescence curve collected on the same
 369 alumina sample just after the plasma exposure and by left the sample under dark for 70 hours after plasma
 370 exposure. The plasma irradiated sample was kept under dark in order to avoid the superposition of
 371 environmental light bleaching to fading effect. In the last case, the glow curve area is about a factor of two
 372 lower with respect to those of the as exposed sample evidencing the presence of the fading effect [15]. Here,
 373 the high temperature glow curve region relates to the initial one since the trap temperature and energy

374 distribution were not modified. Conversely, changes in the temperature and energies of trapped charge
 375 distribution (see Table 2) affect the low temperature glow curve region.



376
 377 **Figure 11.** Thermoluminescence glow curve taken soon after the exposure to plasma and after 70 hours. (colour online)
 378
 379 The fading effect accounts for the high frequency factor S of the lowest temperature peaks indicating that
 380 these traps are more easily released in time and can relax toward a more energetically stable trap distribution.

381
 382 **Table 2.** Peak temperature and energies for glow curves taken just after exposure to plasma, 20, 40 and 70 hours.

	0 hrs	20 hrs	40 hrs	70 hrs
Peak Temperatures (K)				
Pk ₁	390			
Pk ₂	425	429	431	431
Pk ₃	470	469	470	467
		494	494	487
Pk ₄	542	547	547	546
Pk ₅	576	574	576	574
Peak Energies (eV)				
Pk ₁	0.810			
Pk ₂	0.990	1.18	1.31	1.38
Pk ₃	0.760	1.03	1.04	1.14
		1.72	1.82	1.35
Pk ₄	0.640	0.77	0.78	0.76
Pk ₅	0.500	0.50	0.52	0.52

4. Conclusions

Evidence of DBD plasma induced trap filling effect on alumina by using thermoluminescence techniques was clearly observed. The thermoluminescence signal originates from long living traps previously filled by plasma electron current, that are subsequently depleted by heating. The plasma generated thermoluminescence signal was found to be maximum for the Helium glow discharge plasma and in general higher for the homogenous discharge case. Evidence of a strong correlation between the thermoluminescence signal, i.e. the filled electron trap, and the total discharge current charge was demonstrated. Due to the low energy of the plasma electron the penetration depth of the electrons could only be few nanometers, leading to a saturation of the thermoluminescence signal with increasing exposure time. The generated charge traps was observed to last for several days, with a redistribution of the charge on deeper energy level. The redistribution of the trapped charge after several hours from plasma exposure tends to fill higher temperature trap with trap average energy slightly above 1 eV.

Aknowledgments

Authors wish to acknowledge Prof. A. Minafra for fruitful scientific discussion and Mr. G. Casamassima and Mr D. Loiacono for technical support; G.S. and A.C. acknowledge Fondazione Cassa di Risparmio di Puglia Progetto GEOCRONO. This work was possibile thanks to the Laboratorio di Ricerca per la Diagnostica dei Beni Culturali dell'Universita' degli Studi di Bari.

References

-
- [1] M.Li, X.Wang, C.Li,H.Zhan and J.Xu, 2008, *Appl.Phys.Lett* **92**, 031503
 - [2] J Ráhel' and D M Sherman, 2005, *J. Phys. D: Appl. Phys.* **38**, 547
 - [3] Y. B. Golubovskii, V. Maiorov, and J. F. Behnke, 2002, *J. Phys. D*, **35**, 751
 - [4] P. F. Ambrico, M. Ambrico, L. Schiavulli, T. Ligonzo, and V. Augelli, 2009, *Appl. Phys. Lett.* **94**, 051501
 - [5] P. F. Ambrico, M. Ambrico, M. Šimek, A. Colaianne, G. Dilecce, and S. De Benedictis, 2009, *Appl. Phys. Lett.* **94**, 231501
 - [6] A Meiners, M Leck and B Abel, 2009 , *Plasma Sources Sci. Technol.*, **18** 045015
 - [7] H Luo, Z Liang, X Wang, Z Guan and, L Wang , 2010, *J. Phys. D: Appl. Phys.* **43** 155201
 - [8] G Dilecce, P F Ambrico and S De Benedictis, 2007, *Plasma Sources Sci. Technol.* **16** 511
 - [9] F Massines, N Gherardi, N Naudé and P Ségur , 2005 , *Plasma Phys. Control. Fusion* **47** B577
 - [10] I. Radu, R. Bartnikas, M. R. Wertheimer, 2004, *J. Appl. Phys.*, **95**, 5994
 - [11] S. Celestin, G Canes-Boussard, O guaitella, A Bourdon and A Rousseau, 2008, *J. Phys. D: Appl. Phys.*, **41** 205214
 - [12] http://www.risoe.dk/business_relations/Products_Services/Dosimetri/NUK_instruments/TL_OSL_readers.aspx
 - [13] M. Duran, F. Massines, G. Teyssedre, C. Laurent, *Surf. Coat. Tech.*, 2001, **142-144**, 743
 - [14] M. Puchalska, P. Bilski, 2006, *Rad. Meas.* **41**, 659
 - [15] S.W.S. McKeever, *Thermoluminescence of solids*, Cambridge University Press, Cambridge, 1985
 - [16] Chen R and McKeever S W S, *Theory of Thermoluminescence and Related Phenomena*, World Scientific Publishing, Singapore, 1997
 - [17] Horowitz, Y. S. and Yossian, 1995, D., *Radiat. Prot. Dosim.* **60** (1): 3.
 - [18] G. Baldacchini, P. Chiacchiaretta, V. Gupta, V. Kalinov, A. P. Voitovich, 2008, *Phys. Solid State*, **50**, 1747
 - [19] H.G.Balian and N.W.Eddy, 1977, *Nucl.Instrum.Methods* **145** 389
 - [20] H. Kato, K. Soo Seol, M. Fujimaki, T. Toyoda, Y. Ohki and M. Takiyama, 1999, *Jpn. J. Appl. Phys.* **38** 6791
 - [21] H.G.Balian and N.W.Eddy, 1977, *Nucl.Instrum.Methods*, **145** 389
 - [22] J. C. Ashley and V. E. Anderson, 1981, *J. Electron Spectrosc. Relat. Phenom.* **24**, 127
 - [23] J. FaiËn, S. Sanzelle, Th. Pilleyre, D. Miallier, M. Montret, 1999, *Rad. Meas.* **30**, 487